ACADÉMIE
DES SCIENCES
INSTITUT DE FRANCE

Comptes Rendus
Chimie

Ahmed Ould Saleck, Abderrazzak Assani, Mohamed Saadi,
Cyrille Albert-Mercier, Claudine Follet-Houttemane and Lahcen El Ammari

Synthesis and structural study of new phosphates: $AMg_2Fe(PO_4)_3$ (A = Sr or Ba) with the α-$CrPO_4$ structure type

Volume 29 (2026), p. 145-153

Online since: 12 March 2026

https://doi.org/10.5802/crchim.442

The Comptes Rendus. Chimie *are a member of the Mersenne Center for open scientific publishing*
www.centre-mersenne.org — e-ISSN : 1878-1543

ACADÉMIE DES SCIENCES
INSTITUT DE FRANCE

Comptes Rendus. Chimie
2026, Vol. 29, p. 145-153
https://doi.org/10.5802/crchim.442

Research article

Synthesis and structural study of new phosphates: $AMg_2Fe(PO_4)_3$ (A = Sr or Ba) with the α-$CrPO_4$ structure type

Ahmed Ould Saleck[*,a], **Abderrazzak Assani**[b], **Mohamed Saadi**[b], **Cyrille Albert-Mercier**[c], **Claudine Follet-Houttemane**[c] **and Lahcen El Ammari**[b]

[a] Research Unit: Membranes, Matériaux, Environnement et Milieux Aquatiques (2MEMA), BP 5026, FST, Université de Nouakchott, Mauritanie

[b] Laboratoire de Chimie Appliquée des Matériaux, Centre des Sciences des Matériaux, Faculty of Science, Mohammed V University in Rabat, Avenue Ibn Batouta, BP 1014, Rabat, Morocco

[c] Univ. Polytechnique Hauts-de-France, INSA Hauts-de-France, CERAMATHS-Département Matériaux et Procédés, Valenciennes, F-59313, France

E-mail: ahmed.medlemine@univ-nkc.mr (A. Ould Saleck)

Abstract. Single crystals of new orthophosphates $AMg_2Fe(PO_4)_3$ (A = Sr or Ba) have been synthesized by solid-state reaction. From single crystal X-ray diffraction data, their corresponding crystal structures were solved in the orthorhombic system, with the *Imma* space group and unit cell parameters a = 10.3998 (2) Å, b = 13.2000 (2) Å, c = 6.5364 (1) Å for the strontium compound and a = 10.4996 (2) Å, b = 13.2696 (1) Å, c = 6.6330 (2) Å for the barium compound. Both phosphates crystallize with the α-$CrPO_4$ structure type. The crystal structure of both orthophosphates is composed of MgO_6 octahedra, FeO_6 octahedra, and PO_4 tetrahedra. The sharing of vertices between those polyhedra leads to a three-dimensional network defining hexagonal tunnels that are occupied by Sr^{2+} or Ba^{2+} cations.

Keywords. Orthophosphate, Crystal structure, Solid-state reaction, X-ray diffraction, α-$CrPO_4$, Single crystal.

Note. Submitted by invitation as part of the 13th edition of the Moroccan Meetings on Solid State Chemistry (REMCES-13).

Manuscript received 30 May 2025, revised 27 November 2025 and 6 January 2026, accepted 15 January 2026, online since 12 March 2026.

1. Introduction

In the α-$CrPO_4$ structure [1], the Cr^{3+} and P^{5+} cations occupy four special positions of the *Imma* space group. Its corresponding framework is constructed on the basis of [CrO_6] octahedra and [PO_4] tetrahedra, revealing vacant channels along the [100] and [010] axis. Accordingly, this phosphate can be formulated as $A1A2Cr1Cr2_2(PO_4)_3$, with the channel vacant sites represented by A1, A2. As one of our points of interest is to elaborate new α-$CrPO_4$-related open-framework phosphates, we have focused our research on the mixed substitution of di- and/or trivalent cations for Cr1 and/or Cr2. Such a substitution leads to the charge compensation requiring the localization of monovalent or divalent cations in the A1 and/or A2 channels. Hence, using the hydrothermal process, we have managed to isolate new phosphates $Ag_2M_3(HPO_4)(PO_4)_2$ (M = Co or Ni) [2,3], besides the rarely encountered mixed-valence manganese phosphates $MMn(II)Mn(III)_2(PO_4)_3$

[*] Corresponding author

(M = Sr, Ba, or Pb) [4–6]. Moreover, the solid-state reaction technique has allowed us to isolate a variety of new other bi- and trivalent-cations-based phosphates with an α-$CrPO_4$ structure type, namely α-$Na_2Ni_2Fe(PO_4)_3$ [7], $NaCuCr_2(PO_4)_3$ [8], $NaZnCr_2(PO_4)_3$ [9], $BaNi_2Fe(PO_4)_3$ [10–12], and $M'Co_2Fe(PO_4)_3$ (M′ = Sr or Ba) [13,14].

These phosphates exhibit interesting physicochemical properties. For example, $NaCoCr_2(PO_4)_3$ and its isotypes $NaNiCr_2(PO_4)_3$ and $Na_2Ni_2Cr(PO_4)_3$ can serve as cathode materials for sodium-ion batteries, owing to their high discharge capacities of 352, 385, and 368 mAh·g^{-1}, respectively [13]. Recently, Matsaev et al. have reported a novel series of iron-based phosphates, α-$Fe_{1-x}Cr_xPO_4$, adopting the α-$CrPO_4$ structure type, capable of Li-ion intercalation in a high potential region.

The present work is devoted to the synthesis and crystal structure study of the two new magnesium phosphates $AMg_2Fe(PO_4)_3$ (A = Sr or Ba) with the α-$CrPO_4$ structure type.

2. Experimental

2.1. *Crystal growth*

Single crystals of the two compounds $AMg_2Fe(PO_4)_3$ (A = Sr or Ba) were grown by solid-state reaction. The crystals were prepared from a stoichiometric mixture of ACO_3 (A = Sr or Ba) ($BaCO_3$: Sigma-Aldrich, 98%; $SrCO_3$: $BaCO_3$: Seelze–Hannover, 99%), $Mg(NO_3)_2{\cdot}6H_2O$ (Sigma-Aldrich, 97%), $Fe(NO_3)_3{\cdot}9H_2O$ (Panreac, 98%) and $NH_4H_2PO_4$ (Alfa Aesar, 98%). The mixture was progressively heated in a platinum crucible to 573, 673, 773, and 873 K, maintaining each temperature for one night, combined with intermediate grindings. The products were then heated slowly at a rate of 5 °C/min, to 1473 K in the Sr case and to 1353 K for Ba. The final product was maintained at the final temperature for 10 min followed by cooling at room temperature at a rate of 5 °C/h. Finally, green single crystals were isolated from the Sr-containing preparation while brown crystals were obtained with Ba.

2.2. *Crystal structure study*

A single crystal of each preparation was chosen carefully under microscope with suitable dimensions for X-ray diffraction (XRD) studies. The XRD data were collected using a Bruker D8 Venture Super DUO diffractometer with a PHOTON100 CMOS area-detector and monochromatic MoKα radiation (λ = 0.71073 Å) at room temperature. The APEX3 [15] software was used for data collection and the data were integrated with the SAINT-Plus program. Absorption corrections were performed by a multiscan semi-empirical method using SADABS [16]. The two crystal structures were solved by the Patterson method and refined by the SHELXT 2014 [17] and SHELXL 2018 [18] programs incorporated in the WinGX interface [19]. The structural graphics were drawn using the DIAMOND program [20].

3. Results and discussion

Table 1 summarizes the crystal data and structural refinement results. For both structures $AMg_2Fe(PO_4)_3$ (A = Sr or Ba), the refinement of all ions in anisotropy led to good reliability factors (R_1 = 0.018 and wR_2 = 0.047 for $SrMg_2Fe(PO_4)_3$, R_1 = 0.012 and wR_2 = 0.032 for $BaMg_2Fe(PO_4)_3$).

The two compounds crystallize in the *Imma* space group with the following unit cell parameters: a = 10.3998 (2) Å, b = 13.2000 (2) Å, c = 6.5364 (1) Å, and V = 897.30 (3) Å^3 for the strontium-based phosphate and a = 10.4996 (2) Å, b = 13.2696 (1) Å, c = 6.6330 (2) Å, and V = 924.15 (3) Å^3 for the barium-based phosphate.

The atomic coordinates and equivalent isotropic displacement parameters are given in Table 2. The atomic anisotropic displacement parameters are presented in Table 3. The bivalent cation (site = Ba1 or Sr1) is refined in the special position (4*e*). The P^{5+} ions (sites named P1 and P2) are located in the special Wyckoff positions (4*e*) and (8*g*), respectively. Two sites of the O^{2-} ions, named O1 and O2, are refined in the special positions (8*h*) and (8*i*) respectively, while the other O^{2-} ions (O3 and O4 sites) are in the general position (16*j*).

However, the position refinement of cations Fe^{3+} and Mg^{2+} in the special positions (4*e*) and (8*g*), respectively, results in negative atomic displacement parameters for Mg^{2+}, a high-density residue in the vicinity of Mg^{2+}, and a density deficit in the vicinity of Fe^{3+}, despite the very good R_1 and wR_2 factors obtained. Those facts suggest the concomitant localization of Fe^{3+} and Mg^{2+} in the same site.

Table 1. Crystal data and structure refinement of $AMg_2Fe(PO_4)_3$ (A = Sr or Ba)

Compound	$SrMg_2Fe(PO_4)_3$	$BaMg_2Fe(PO_4)_3$
Crystal data		
Crystal system	Orthorhombic	Orthorhombic
Space group	*Imma*	*Imma*
Cell dimension (Å)	10.3998 (2)	10.4996 (2)
	13.2000 (2)	13.2696 (1)
	6.5364 (1)	6.6330 (2)
Cell volume (Å^3)	897.30 (3)	924.15 (3)
Multiplicity Z	4	4
Molecular weight (g/mol)	477	526.72
Density (g/cm^{-3})	3.531	3.786
Coefficient absorption μ (mm^{-1})	8.31	6.53
Data collection		
Diffractometer	Brüker X8 APEX- CCD	Brüker X8 APEX- CCD
No. of measured, independent, and observed [$I \geq 2\sigma(I)$] reflections	9561, 892, 876	22556, 1671, 1595
R_{int}	0.035	0.032
θ_{min}–θ_{max} (°)	3.1–32.5	3.1–41.5
Refinement		
$R[F^2 > 2\sigma(F^2)]$	0.018	0.012
$wR_2(F^2)$	0.047	0.032
S (Goodness-of-Fit):	1.19	1.16
No of refined parameters	54	58
No. of restraints	0	
$\Delta\rho_{max}, \Delta\rho_{min}$ (e·Å^{-3})	0.58, −0.82	1.38, −1.03

Such an assumption is established by the last refinement assuming, firstly, the localization of both Fe^{3+} and Mg^{2+} in the same crystallographic Wyckoff position (4*a*), initially assigned only to Fe^{3+}. The occupancy rate obtained in this site, hereafter named Fe1/Mg1 site, corresponds to 0.880 (1) for Fe^{3+} and 0.120 (1) for Mg^{2+} in the strontium compound. Likewise, the remaining amount of Fe accommodates the site of Mg2 at the special Wyckoff position (8*g*), hereafter called Mg2/Fe2 site in the strontium phosphate. Such refinement led to an occupancy of 0.940 (1) for Mg^{2+} and 0.060 (1) for Fe^{3+} at the Mg2/Fe2 site. Therefore, refining the Fe/Mg site occupancy ratios in the case of the Sr compound, taking into account the electrical neutrality of the molecule, leads to a stoichiometric compound with a Mg/Fe ratio of two and therefore a $SrMg_2Fe(PO_4)_3$ formula. In contrast, in the case of the Ba compound, the Mg/Fe ratio is slightly less than two (7.482 (1)/4.518 (1)), and the electrical neutrality of the molecule is no longer maintained. This can be explained by the presence of a small amount of Fe^{2+}, and consequently, the formula of the resulting compound will be $BaMg_{1.87}Fe_{0.13}Fe(PO_4)_3$.

Selected bond lengths and angles in both compounds $AMg_2Fe(PO_4)_3$ (A = Sr or Ba) are listed in Table 4.

In the two compounds $SrMg_2Fe(PO_4)_3$ and $BaMg_2Fe(PO_4)_3$, the P^{5+} ions located at the Wyckoff positions (4*e*) and (8*g*) for P1 and P2 sites, respectively, have a tetrahedral environment ($P1O_4$ and $P2O_4$) with a mean distance ⟨P–O⟩ of 1.540 Å.

Table 2. Atomic coordinates, occupancies, and equivalent isotropic displacement parameters (Å^2) of $SrMg_2Fe(PO_4)_3$ and $BaMg_2Fe(PO_4)_3$*

Atom	Site	Occupation	x	y	z	$U_{éq}$
Sr1	$4e$	1	0.0000	0.7500	0.59942 (3)	0.00871 (8)
Ba1*			0.0000	0.7500	0.60778 (2)	0.00789 (4)
Fe1/Mg1	$4a$	0.880 (1)/0.120 (1)	0.5000	0.5000	0.5000	0.00398 (9)
Fe1/Mg1*		0.871 (1)/0.129 (1)	0.5000	0.5000	0.5000	0.00384 (5)
Mg2/Fe2	$8g$	0.940 (1)/0.060 (1)	0.7500	0.63349 (4)	0.2500	0.0053 (1)
Mg2/Fe2*		0.871 (1)/0.129 (1)	0.7500	0.63293 (3)	0.2500	0.00283 (7)
P1	$4e$	1	0.0000	0.7500	0.09209 (8)	0.0038 (1)
P1*			0.0000	0.7500	0.10104 (8)	0.00341 (8)
P2	$8g$	1	0.7500	0.42840 (3)	0.2500	0.0043 (1)
P2*			0.7500	0.42840 (3)	0.2500	0.0043 (1)
O1	$8h$	1	0.0000	0.65613 (9)	−0.0436 (2)	0.0071 (2)
O1*			0.0000	0.65524 (8)	−0.0294 (2)	0.0065 (2)
O2	$8i$	1	0.8822 (1)	0.7500	0.2362 (2)	0.0064 (2)
O2*			0.8813 (1)	0.7500	0.2390 (2)	0.0059 (2)
O3	$16j$	1	0.71114 (9)	0.36450 (7)	0.0665 (1)	0.0081 (2)
O3*			0.71689 (9)	0.36643 (6)	0.0661 (1)	0.0082 (1)
O4	$16j$	1	0.63860 (8)	0.50528 (6)	0.2950 (1)	0.0062 (2)
O4*			0.63800 (7)	0.50498 (6)	0.2930 (1)	0.0062 (1)

Table 3. Anisotropic displacement parameters (Å^2) of $SrMg_2Fe(PO_4)_3$ and $BaMg_2Fe(PO_4)_3$*

Atom	U^{11}	U^{22}	U^{33}	U^{12}	U^{13}	U^{23}
Sr1	0.0091 (1)	0.0114 (1)	0.0056 (1)	0.000	0.000	0.000
Ba1*	0.00716 (6)	0.01205 (6)	0.00447 (5)	0.000	0.000	0.000
Fe1/Mg1	0.0034 (2)	0.0041 (2)	0.0044 (2)	0.000	0.000	0.0003 (1)
Fe1/Mg1*	0.0034 (1)	0.0040 (1)	0.0041 (1)	0.000	0.000	0.00011 (8)
Mg2/Fe2	0.0051 (2)	0.0040 (2)	0.0067 (2)	0.000	0.0002 (2)	0.000
Mg2/Fe2*	0.0027 (2)	0.0013 (2)	0.0045 (2)	0.000	0.0003 (1)	0.000
P1	0.0038 (2)	0.0034 (2)	0.0043 (2)	0.000	0.000	0.000
P1*	0.0033 (2)	0.0033 (2)	0.0036 (2)	0.000	0.000	0.000
P2	0.0047 (2)	0.0038 (2)	0.0044 (2)	0.000	0.0005 (1)	0.000
P2*	0.0040 (1)	0.0039 (1)	0.0040 (1)	0.000	0.0005 (1)	0.000
O1	0.0088 (5)	0.0050 (5)	0.0074 (5)	0.000	0.000	−0.0018 (4)
O1*	0.0086 (4)	0.0039 (3)	0.0069 (4)	0.000	0.000	−0.0018 (3)
O2	0.0051 (5)	0.0071 (5)	0.0070 (5)	0.000	0.0015 (4)	0.000
O2*	0.0042 (4)	0.0076 (3)	0.0059 (4)	0.000	0.0016 (3)	0.000
O3	0.0101 (4)	0.0074 (4)	0.0067 (3)	−0.0018 (3)	0.0002 (3)	−0.0022 (3)
O3*	0.0096 (3)	0.0085 (3)	0.0065 (3)	−0.0021 (2)	0.0003 (2)	−0.0027 (2)
O4	0.0053 (3)	0.0059 (3)	0.0075 (3)	0.0012 (3)	0.0015 (3)	0.0006 (3)
O4*	0.0047 (3)	0.0064 (2)	0.0073 (3)	0.0011 (2)	0.0017 (2)	0.0008 (2)

Table 4. Interatomic distances (Å) and angles (°) for $AMg_2Fe(PO_4)_3$ (A = Sr or Ba)

P–O distances (Å) and O–P–O angles (°)		
Distance (Å)	$SrMg_2Fe(PO_4)_3$	$BaMg_2Fe(PO_4)_3$
P1–O1	1.524 (1)	1.526 (1)
P1–O1^{ix}	1.524 (1)	1.526 (1)
P1–O2^{ix}	1.546 (1)	1.546 (1)
P1–O2	1.546 (1)	1.546 (1)
Average distances	1.535	1.536
P2–O3	1.521 (1)	1.521 (1)
P2–O3^{vii}	1.521 (1)	1.521 (1)
P2–O4^{vii}	1.568 (1)	1.570 (8)
P2–O4	1.568 (1)	1.570 (8)
Average distances	1.544	1.545
Angle (°)	$SrMg_2Fe(PO_4)_3$	$BaMg_2Fe(PO_4)_3$
O1–P1–O1^{ix}	108.8 (1)	109.61 (3)
O1–P1–O2^{ix}	110.77 (3)	110.94 (9)
O1^{ix}–P1–O2^{ix}	110.77 (3)	109.61 (3)
O1–P1–O2	110.77 (3)	109.61 (3)
O1^{ix}–P1–O2	110.77 (3)	109.61 (3)
O2^{ix}–P1–O2	104.91 (9)	107.40 (9)
O3–P2–O3^{vii}	112.62 (7)	112.15 (4)
O3–P2–O4^{vii}	114.04 (5)	113.05 (7)
O3^{vii}–P2–O4^{vii}	108.10 (5)	109.00 (5)
O3–P2–O4	108.10 (5)	109.00 (5)
O3^{vii}–P2–O4	114.04 (5)	112.15 (4)
O4^{vii}–P2–O4	99.34 (7)	100.87 (6)
Fe1/Mg1–O distances (Å) and O–Fe1/Mg1–O angles (°)		
Distance (Å)	$SrMg_2Fe(PO_4)_3$	$BaMg_2Fe(PO_4)_3$
Fe1/Mg1–O4^{i}	1.9692 (8)	1.9975 (8)
Fe1/Mg1–O4^{ii}	1.9692 (8)	1.9975 (8)
Fe1/Mg1–O4^{iii}	1.9692 (8)	1.9975 (8)
Fe1/Mg1–O4	1.9692 (8)	1.9975 (8)
Fe1/Mg1–O1^{iv}	2.081 (1)	2.069 (1)
Fe1/Mg1–O1^{v}	2.081 (1)	2.069 (1)
Average distances	2.007	2.021
Angle (°)	$SrMg_2Fe(PO_4)_3$	$BaMg_2Fe(PO_4)_3$
O1^{iv}–Fe1/Mg1–O1^{v}	180.0	180.000 (6)
O4^{ii}–Fe1/Mg1–O1^{v}	86.67 (3)	88.18 (3)
O4^{i}–Fe1/Mg1–O1^{v}	93.33 (3)	91.82 (3)
O4^{iii}–Fe1/Mg1–O1^{v}	93.33 (3)	91.82 (3)

(continued on next page)

Table 4. (continued)

O4–Fe1/Mg1–O1^{v}	86.67 (3)	88.18 (3)
O4–Fe1/Mg1–O1^{iv}	93.33 (3)	91.82 (3)
O4^{i}–Fe1/Mg1–O1^{iv}	86.67 (3)	88.18 (3)
O4^{iii}–Fe1/Mg1–O1^{iv}	86.67 (3)	88.18 (3)
O4^{ii}–Fe1/Mg1–O1^{iv}	93.33 (3)	91.82 (3)
O4^{i}–Fe1/Mg1–O4	85.90 (5)	87.00 (5)
O4^{i}–Fe1/Mg1–O4^{iii}	94.10 (5)	93.00 (5)
O4^{ii}–Fe1/Mg1–O4^{iii}	85.90 (5)	87.00 (5)
O4^{ii}–Fe1/Mg1–O4	94.10 (5)	93.00 (5)

Mg2/Fe2–O distances (Å) and O–Mg2/Fe2–O angles (°)

Distance (Å)	$SrMg_2Fe(PO_4)_3$	$BaMg_2Fe(PO_4)_3$
Mg2/Fe2–O2	2.0647 (9)	2.0784 (8)
Mg2/Fe2–O2^{vi}	2.0647 (9)	2.0784 (8)
Mg2/Fe2–O4	2.0719 (9)	2.0849 (9)
Mg2/Fe2–O4^{vii}	2.0719 (9)	2.0849 (9)
Mg2/Fe2–O3^{v}	2.1083 (9)	2.1252 (8)
Mg2/Fe2–O3^{viii}	2.1083 (9)	2.1252 (8)
Average distances	2.082	2.096
Angle (°)	$SrMg_2Fe(PO_4)_3$	$BaMg_2Fe(PO_4)_3$
O3^{v}–Mg2/Fe2–O3^{viii}	178.56 (6)	179.55 (5)
O4–Mg2/Fe2–O3^{v}	88.74 (4)	87.75 (3)
O4^{vii}–Mg2/Fe2–O3^{v}	92.44 (4)	92.62 (3)
O2–Mg2/Fe2–O3^{v}	84.60 (4)	85.59 (4)
O2^{vi}–Mg2/Fe2–O3^{v}	94.32 (4)	94.07 (4)
O4–Mg2/Fe2–O3^{viii}	92.44 (4)	92.62 (3)
O4^{vii}–Mg2/Fe2–O3^{viii}	88.74 (4)	87.75 (3)
O2–Mg2/Fe2–O3^{viii}	94.32 (4)	94.07 (4)
O2^{vi}–Mg2/Fe2–O3^{viii}	84.60 (4)	85.59 (4)
O4–Mg2/Fe2–O4^{vii}	70.47 (5)	70.95 (4)
O2–Mg2/Fe2–O4^{vii}	103.29 (3)	103.28 (3)
O2–Mg2/Fe2–O2^{vi}	83.70 (5)	83.27 (5)
O2^{vi}–Mg2/Fe2–O4	103.29 (3)	103.28 (3)

A1–O distances (Å) (A1 = Sr or Ba)

Distance (Å)	$SrMg_2Fe(PO_4)_3$	$BaMg_2Fe(PO_4)_3$
A1–O1^{xi}	2.642 (1)	2.715 (1)
A1–O2	2.672 (1)	2.715 (1)
A1–O2^{ix}	2.672 (1)	2.745 (1)
A1–O3^{v}	2.6744 (9)	2.745 (1)
A1–O3^{xii}	2.6744 (9)	2.7658 (9)

(continued on next page)

Table 4. (continued)

A1–O3^{xiii}	2.6744 (9)	2.7658 (9)
A1–O3^{xiv}	2.6744 (9)	2.7658 (9)
A1–O1^{xi}	2.642 (1)	2.7658 (9)
Average distances	2.666	2.740

Symmetry codes: (i) $x, -y+1, -z+1$; (ii) $-x+1, y, z$; (iii) $-x+1, -y+1, -z+1$; (iv) $x-1/2, y, -z+1/2$; (v) $-x+3/2, -y+1, z+1/2$; (vi) $-x+3/2, -y+3/2, -z+1/2$; (vii) $-x+3/2, y, -z+1/2$; (viii) $x, -y+1, -z$; (ix) $-x+2, -y+3/2, z$; (x) $-x+2, -y+3/2, z+1$; (xi) $x, y, z+1$; (xii) $-x+3/2, y+1/2, z+1/2$; (xiii) $x+1/2, y+1/2, z+1/2$; (xiv) $x+1/2, -y+1, z+1/2$.

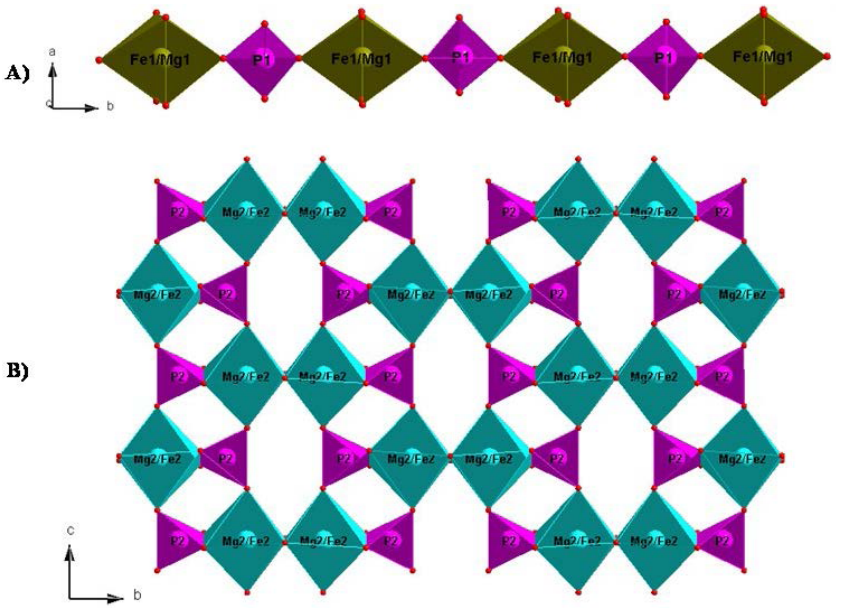

Figure 1. (A) Infinity chain of (Fe1/Mg1)P1O$_9$ formed by sharing vertices of [Fe1Mg1O$_6$] octahedra and P1O$_4$ tetrahedra (B) Sheet showing the (Mg2/Fe2)$_4$P2$_4$O$_{26}$ unit along [010].

In both phosphates AMg$_2$Fe(PO$_4$)$_3$ (A = Sr or Ba), the cations Fe^{3+} and Mg^{2+} located in the Fe1/Mg1 site, corresponding to the crystallographic Wyckoff position (4*a*), are surrounded by six O^{2-} ions forming an octahedron (Fe1/Mg1)O$_6$ with a mean distance ⟨Fe1/Mg1–O⟩ of 2.007 Å for SrMg$_2$Fe(PO$_4$)$_3$ and 2.021 Å for BaMg$_2$Fe(PO$_4$)$_3$.

For the Mg2/Fe2 site, the Mg^{2+} and Fe^{3+} cations are statistically distributed in the Wyckoff position (8*g*) and adopt an octahedral environment (Mg2/Fe2)O$_6$ with a mean distance ⟨Mg2/Fe2–O⟩ of 2.082 Å for SrMg$_2$Fe(PO$_4$)$_3$ and 2.096 Å for BaMg$_2$Fe(PO$_4$)$_3$.

Finally, for each compound, the A cation (Sr^{2+} or Ba^{2+}) is surrounded by eight O^{2-} ions with a distance A–O ranging from 2.642(1) Å to 2.674 (1) Å for SrMg$_2$Fe(PO$_4$)$_3$ and from 2.715 (1) Å to 2.766 (1) Å for BaMg$_2$Fe(PO$_4$)$_3$.

In the crystal structure of AMg$_2$Fe(PO$_4$)$_3$ phosphates (A = Sr or Ba), (Fe1/Mg1)O$_6$ octahedra and P1O$_4$ tetrahedra are connected via common vertices O1 alternately to form linear infinite chains (Fe1/Mg1)P1O$_9$ along the *b* axis (Figure 1A), while the octahedra (Mg2/Fe2)O$_6$ share the O2–O2 edge to form dimers (Mg2/Fe2)$_2$O$_{10}$. Each dimer (Mg2/Fe2)$_2$O$_{10}$ is linked to the two tetrahedral

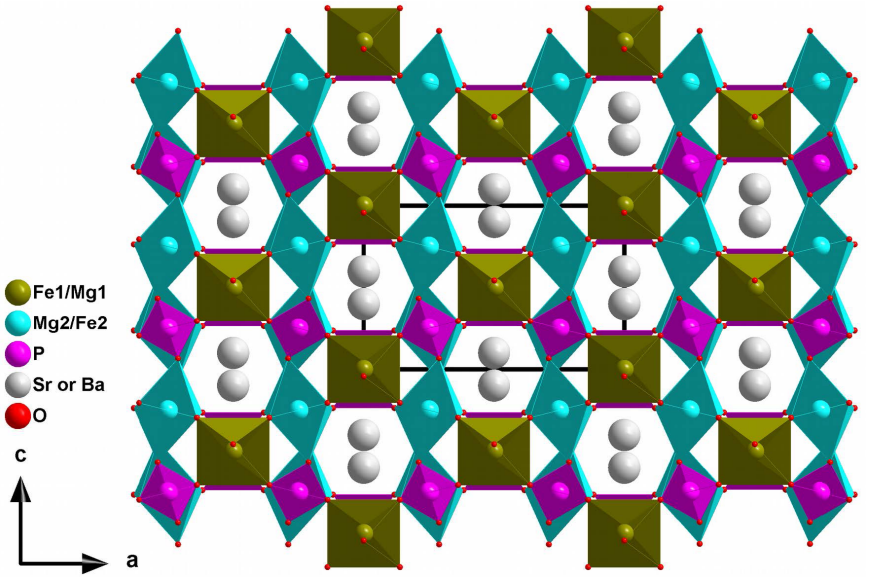

Figure 2. Projection view along the *b* direction of the structure showing the hexagonal tunnels that accommodate Sr or Ba in $AMg_2Fe(PO_4)_3$ (A = Sr or Ba).

groups $P2O_4$ by an O4–O4 edge to form the entity $(Mg2/Fe2)_2P2_2O_{14}$. Those later entities share the O3 vertices to form sheets $(Mg2/Fe2)_4P2_4O_{26}$ parallel to the (*ac*) plane (Figure 1B).

Vertices shared between sheets and chains lead to a three-dimensional framework delimiting two types of tunnels in which the Sr^{2+} or Ba^{2+} cations are located (Figure 2).

Exploration of the crystallographic database shows that the structures of both orthophosphates are similar to structures of the α-$CrPO_4$ type mentioned in literature such as $SrNi_2Fe(PO_4)_3$ [11], $SrCo_2Fe(PO_4)_3$ [13], $SrMn^{II}_2Mn^{III}(PO_4)_3$ [4], $BaNi_2Fe(PO_4)_3$ [10], and $BaMn^{II}_2Mn^{III}(PO_4)_3$ [5].

4. Conclusion

The single crystal X-ray diffraction study of these two new orthophosphates, $SrMg_2Fe(PO_4)_3$ and $BaMg_2Fe(PO_4)_3$ showed that these compounds crystallize in an orthorhombic system (*Imma* space group) with unit cell parameters a = 10.3998 (2) Å, b = 13.2000 (2) Å, c = 6.5364 (1) Å for the strontium compound and a = 10.4996 (2) Å, b = 13.2696 (1) Å, c = 6.6330 (2) Å for the barium composition. Their structures are isotype to α-$CrPO_4$. The crystal structure of both compounds is composed of MgO_6 octahedra, FeO_6 octahedra, and PO_4 tetrahedra. The sharing of vertices between those polyhedra leads to a three-dimensional network delimiting hexagonal channels that are occupied by Ba^{2+} or Sr^{2+} cations.

CRediT authorship contribution statement

Ahmed Ould Saleck: Investigation, Writing—Original draft, Writing—Review & editing.
Claudine Follet-Houttemane: Investigation, Writing—Original draft, Writing—Review & editing.
Cyrille Albert-Mercier: Investigation, Writing—Original draft, Writing—Review & editing.
Lahcen El Ammari: Formal analysis, Writing—Original draft, Writing—Review & editing.
Mohamed Saadi: Formal analysis, Writing—Original draft, Writing—Review & editing.
Abderrazzak Assani: Formal analysis, Writing—Original draft, Writing—Review & editing.

Declaration of interests

The authors do not work for, advise, own shares in, or receive funds from any organization that could benefit from this article, and have declared no affiliations other than their research organizations.

Data availability

All the data generated or analyzed during this study are included in this published article.

The data can be obtained free of charge from the Cambridge Crystallographic Data Centre at http://www.ccdc.cam.ac.uk/structures with deposition number CCDC 2454547 for $BaMg_2Fe(PO_4)_3$ and CCDC 2454549 for $SrMg_2Fe(PO_4)_3$.

References

[1] J. P. Attfield, A. W. Sleight and K. C. Antonie, "Structure determination of α-$CrPO_4$ from powder synchrotron X-ray data", *Nature* **322** (1986), no. 6080, pp. 620–622.

[2] A. Assani, L. El Ammari, M. Zriouil and M. Saadi, "Disilver (I) tricobalt (II) hydrogenphosphate bis(phosphate), $Ag_2Co_3(HPO_4)(PO_4)_2$", *Acta Crystallogr. E* **67** (2011), p. i41.

[3] A. Assani, L. El Ammari, M. Zriouil and M. Saadi, "Disilver (I) trinickel (II) hydrogenphosphate bis (phosphate), $Ag_2Ni_3(HPO_4)(PO_4)_2$", *Acta Crystallogr. E* **67** (2011), p. i40.

[4] G. Alhakmi, A. Assani, M. Saadi, C. Follet and L. El Ammari, "$SrMn^{II}_2Mn^{III}(PO_4)_3$", *Acta Crystallogr. E* **69** (2013), p. i56.

[5] A. Assani, M. Saadi, G. Alhakmi, E. Houmadi and L. El Ammari, "$BaMn^{II}_2Mn^{III}(PO_4)_3$", *Acta Crystallogr. E* **69** (2013), p. i60.

[6] G. Alhakmi, A. Assani, M. Saadi and L. El Ammari, "A new mixed-valence lead (II) manganese (II/III) phosphate (V): $PbMn^{II}_2Mn^{III}(PO_4)_3$", *Acta Crystallogr. E* **69** (2013), p. i40.

[7] R. Essehli, I. Belharouak, H. Ben Yahia, et al., "α-$Na_2Ni_2Fe(PO_4)_3$: a dual positive/negative electrode material for sodium ion batteries", *Dalton Trans.* **44** (2015), no. 10, pp. 4526–4532.

[8] K. Souiwa, E. Lebraud, M. Gayot, et al., "Structural and spectroscopic studies of $NaCuCr_2(PO_4)_3$: a noncentrosymmetric phosphate belonging to the α-$CrPO_4$-type compounds", *Inorg. Chem.* **60** (2021), no. 11, pp. 7803–7814.

[9] K. Souiwa, M. Hidouri, O. Toulemonde, M. Duttine and M. B. Amara, "Synthesis and characterization of the phosphates Na1 + $x$$Mg_{1+x}Cr_{2-x}(PO_4)_3$ (x = 0; 0.2) and $NaZnCr_2(PO_4)_3$ with the α-$CrPO_4$ structure", *J. Alloys Compd.* **627** (2015), pp. 153–160.

[10] S. Ouaatta, A. Bouraima, E. Benhsina, J. Khmiyas, A. Assani, M. Saadi and L. El Ammari, "Crystal structure of barium dinickel(II) iron(III) tris[orthophosphate(V)], $BaNi_2Fe(PO_4)_3$", *Acta Crystallogr. E* **79** (2023), no. 2, pp. 95–98.

[11] A. Bouraima, T. Makani, A. Assani, M. Saadi and L. El Ammari, "Crystal structure of strontium dicobalt iron(III) tris(orthophosphate): $SrCo_2Fe(PO_4)_3$", *Acta Crystallogr. E* **72** (2016), pp. 1143–1146.

[12] A. Bouraima, J. J. Anguile, A. Assani, M. Saadi, T. Makani and L. El Ammari, "Crystal structure of baryum dicobalt iron (III) tris(Orthophosphate) belonging to α-$CrPO_4$ family", *Open J. Inorg. Chem.* **10** (2020), no. 1, pp. 1–5.

[13] H. Ben Yahia, R. Essehli, M. Avdeev, J. B. Park, Y. K. Sun, M. A. Al-Maadeed and I. Belharouak, "Neutron diffraction studies of the Na-ion battery electrode materials $NaCoCr_2(PO_4)_3$, $NaNiCr_2(PO_4)_3$, and $Na_2Ni_2Cr(PO_4)_3$", *J. Solid State Chem.* **238** (2016), pp. 103–108.

[14] B. A. Matsaev, N. D. Luchinin, I. A. Trussov, et al., "Synthesis and reversible Li-ion intercalation of a novel chromium-doped iron phosphate with an α-$CrPO_4$ structure", *J. Mater. Chem. A* **13** (2025), no. 25, pp. 19911–19922.

[15] L. Bruker, *APEX3 (Version 5.054), SAINT + (Version 6.36A)*, Bruker AXS Inc.: Madison, WI, 2016.

[16] L. Krause, R. Herbst-Irmer, G. M. Sheldrick and D. Stalke, "Comparison of silver and molybdenum microfocus X-ray sources for single-crystal structure determination", *J. Appl. Crystallogr.* **48** (2015), pp. 3–10.

[17] G. M. Sheldrick, "SHELXT—Integrated space-group and crystal-structure determination", *Acta Crystallogr. A* **71** (2015), pp. 3–8.

[18] G. M. Sheldrick, "Crystal structure refinement with SHELXL", *Acta Crystallogr. C* **71** (2015), pp. 3–8.

[19] L. J. Farrugia, "WinGX and ORTEP for windows: an update", *J. Appl. Crystallogr.* **45** (2012), pp. 849–854.

[20] G. Bergerhoff, M. Berndt and K. Brandenburg, "Evaluation of crystallographic data with the program DIAMOND", *J. Res. Natl. Inst. Stand. Technol.* **101** (1996), pp. 21–25.